EXPLOSION SOURCE PHENOMENA USING SOVIET TEST ERA WAVEFORM DATA

Tatyana G. Rautian[1], Vitaly I. Khalturin[1], W. Scott Phillips[2], and Paul G. Richards[1]

Columbia University[1], Los Alamos National Laboratory[2]

Sponsored by National Nuclear Security Administration
Office of Nonproliferation Research and Engineering
Office of Defense Nuclear Nonproliferation

Contract No. DE-FC52-03NA99513[1], W-7405-ENG-36[2]

ABSTRACT

During the nuclear testing era, the former Soviet Union carried out extensive observations of underground nuclear explosions, recording both their own shots and those of foreign nuclear states. Between 1961 and 1989, the Soviet "Complex Seismological Expedition" deployed seismometers at time-varying subsets of over 150 sites to record explosions at regional distances from the Semipalatinsk and Lop Nor test sites and from the shot points of peaceful nuclear explosions. This data set included recordings from broadband, multi-channel ChISS[1] seismometers that produced a series of narrow band outputs, which could then be measured to perform spectral studies. Quantitative, pre-digital era investigations of high-frequency source scaling relied on this type of data (e.g., Aki and Chouet, 1975; Rautian and Khalturin, 1978; Tsujiura, 1978). To augment data sets of Central Asia explosions, we have measured and compiled 537 ChISS coda envelopes for 124 events recorded at Talgar, Kazakhstan, at a distance of about 750 km from Semipalatinsk. Envelopes and calibration levels were measured manually from photo paper records for seven bands between 0.08 and 5 Hz. We obtained from 2 to 10 coda envelope measurements per event, depending on the event size and instrument magnification. Coda lengths varied from 250 to 1400 s. For small events, only bands between 0.6 and 2.5 Hz could be measured. Envelope levels were interpolated or extrapolated to 500 s and we have obtained the dependence of this quantity on magnitude. Coda Q was estimated and found to increase from 232 at 0.08 Hz to 1270 at 5 Hz. These relationships were used to construct an average scaling law of coda spectra for Semipalatinsk explosions. Significant differences from average scaling are observed and may result from variations in emplacement conditions. The ChISS envelope data will be integrated into coda processing at Los Alamos National Laboratory (LANL) by applying ChISS filter bands to modern, digital data from Central Asia, for purposes of magnitude and yield calibration.

[1] ChISS is the Russian abbreviation for multichannel spectral seismometer. In this instrument the signal from the seismometer is passed through a system of narrow bandpass filters and recorded on photo paper. ChISS instruments have from 8 to 16 channels in the frequency range from 100 sec to 40 Hz. We used data mostly from 7 channels, ranging from 0.08 to 5 Hz.

OBJECTIVE

Our objective is to augment the collection of seismic recordings of Central Asia underground nuclear tests and test-site earthquakes using ChISS data collected at Talgar, Kazakhstan, between 1961 and 1989; and to integrate these data into coda wave processing schemes currently in use with modern digital data. This will greatly increase the numbers of events used in explosion source scaling and yield estimation studies for the Semipalatinsk Test Site. Furthermore, data from rare earthquakes on and near the Semipalatinsk Test Site will be useful to test calibration parameters currently applied to amplitude data from that test site.

RESEARCH ACCOMPLISHED

The ChISS Instrument

The ChISS instrument is a real-time, spectral-analyzing seismic recording system, created by K.K. Zapolsky in the early 1950s. It produced band-passed traces in several (usually 7-10) frequency channels over a broad band from 100 seconds to 40 Hz. The components of a ChISS system are the seismometer, calibration device, amplifier, filter bank, and galvanometers with a photo-paper recording device. Instrument calibration was achieved by each seismometer having an excitation coil with a separate magnet to input the calibration signal. The frequency of the calibration electric signal was slowly decreased in time from the high end of the highest frequency filter to the low end of the lowest frequency filter. The shape of the response to this signal on the seismogram exactly corresponds to the frequency response of the seismometer-filter-galvanometer system. The impulse response consists of 1.5-2 periods (3-4 extrema). Such a short period of transition guarantees minimal distortion of the initial seismic signal and stabilizes the envelope shape. Filters used in ChISS systems are characterized by the low and high band limits (at 0.7 maximum magnification), f1 and f2; the central frequency, fc; the absolute bandwidth, df = f2 - f1; and the relative bandwidth, (f2 - f1)/fc.

The ChISS filter parameters at the Talgar station used in this study are shown in Tables 1 and 2. Parameters were changed in September 1971 when the system was improved to include two sets of filters for independent short-period (ShP) and long-period (LP) seismometers, as well as independent systems of calibration and recording. The LP and ShP ChISS instruments employ Soviet SKD and SKM seismometers, respectively. Two identical ChISS filters, with central frequency 0.62 Hz, are output from both systems. The calibration signal was recorded daily on each short period ChISS seismogram and once a week on long period ChISS seismograms.

Table 1. Early ChISS parameters (Sep 1961 – Aug 1971)

f1 - f2 (Hz)	0.27-0.4	0.54-0.84	1.1-1.7	2.3-3.6	4.6-7.1
fc (Hz)	0.32	0.67	1.36	2.9	5.7
Width	0.40	0.45	0.45	0.45	0.45

Table 2. Standard ChISS parameters (Sep 1971 – Oct 1990)

LP or ShP	LP	LP	LP	LP	ShP	ShP	ShP	ShP
f1 - f2 (Hz)	0.05-0.1	0.1-0.2	0.2-0.4	0.5-0.8	0.5-0.8	1.0-1.6	2.0-3.2	4-6.4
fc (Hz)	0.08	0.14	0.28	0.62	0.62	1.25	2.5	5.0
Width	0.7	0.7	0.7	0.5	0.5	0.5	0.5	0.5

Talgar Explosion Data

The Talgar ChISS station began operating in September 1961. It recorded almost all Soviet underground nuclear tests (UNTs) from the Semipalatinsk test site (STS), including the first two STS UNTs on Oct 11, 1961 and Feb 2, 1962 until the final test of Oct 19, 1989. Many small magnitude UNTs, which were not recognized by western stations, have been recorded by ChISS station TLG (Khalturin et al., 2001).

For this study, we manually measured coda envelopes of 178 Talgar ChISS records of 124 UNTs and entered the data into the computer. More than 500 coda envelopes were analyzed from channels between 0.08 Hz and 5 Hz.

For measurable channels, the number of coda amplitudes obtained varied from 3-5 to 10-12, depending on the intensity of event and magnification of instrumentation. For small events only two or three channels had records with coda large enough to be measured, generally 0.62, 1.25 and 2.5 Hz. For large events five, six and up to eight channels were measurable. Elapsed time relative to the event origin varied from 250 seconds to as much as 1,400 seconds in some cases.

Observed Direct and Coda Phases

We consider the coda as consisting of two parts. The first portion is the tail of the dominant direct wave, originating from scattering in the vicinity of the ray path. The second portion is the "late coda" or "coda" originating from scattering throughout a large volume of the Earth, of a dimension greater than the epicentral distance. Excitation of the late coda is insensitive to path variations, but depends on variations in spectral content radiated by each individual event. For this reason, we rely on the late coda to study spectral scaling and explosion emplacement conditions.

We must define the time at which the late coda begins, which entails detailed investigation of the dominant direct waves preceding the coda. We observe three intensive waves along the STS-Talgar path: 1) the ***Lg*** wave train, arriving at Talgar at 210-215 seconds, reaching maximum intensity at about 220-240 seconds and remaining intense until 250-270 sec; 2) the ***Rg***, arriving at 240 sec, with maximum at 260-270 sec and intense until 300 sec; and 3) the ***Lo***, which is a wave group observed in the 340-450 second time interval, perhaps a short-period surface wave train with group velocity 1.9-2.2 km/sec, observed on the 0.28 - 1.25 Hz channels with amplitude just above the coda. The ***Lo*** group is weaker than ***Rg*** on long-period channels, and weaker than ***Lg*** on short-period channels. At mid-period channels, 0.28 and 0.32 Hz, ***Lg***, ***Rg*** and ***Lo*** have roughly equal amplitudes. Each of these waves produces its own coda, which overlaps with coda of the other phases.

Aki's "rule of thumb" for coda measurement defines the beginning of the late coda as twice the travel time of the associated direct wave. In reality the factor of two can vary. We find the critical time empirically for our study. This is done based on observations of the envelope shapes, including both early and late coda. We began to measure the envelope soon after the passage of ***Lg*** or ***Rg*** waves.

To manually obtain the coda envelope from a photo paper record, one must choose each individual moment of time to measure. We chose measurement times such that monotonically decreasing amplitudes are obtained. Strict adherence to this rule enhances repeatability, which we have verified by comparing measurements obtained independently by two analysts. Further testing has shown that measurements from the short and long period recording in the common, 0.62 Hz, band are the same.

The accuracy of manual measurements of ChISS envelopes depends on amplitude. The accuracy is lower for small amplitudes (below 1-2 mm) and large amplitudes (over 70-100 mm). Our estimate is that amplitudes less than 1 mm can be measured with error on the order of the amplitude itself. Therefore we eliminate all data below this level. The difficulty with large amplitudes is that waveforms from neighboring channels can overlap. Channels are recorded side by side and are separated by 70 mm; thus, peak-peak amplitudes larger than 70-100 mm overlap. From our experience, measurement quality depends on brightness of the record.

Occasionally, errors result from mistakes in measuring calibration levels. In such cases, both coda and direct wave amplitudes have the same discrepancy for that channel. This cannot be seen in individual envelopes, but is revealed in the spectra of individual events and in correlations between amplitude and magnitude. Such comparisons have been made to control the quality of the Talgar data set.

We summarize observations of the coda envelopes by band in the following. All the individual envelopes were normalized to the level 1 at lapse time 500 seconds. The bands of f = 0.62 Hz from the LP and ShP ChISS systems were combined together. The envelopes (Figures 1a,b,c,d,e,f) are corrected for geometrical spreading, assumed to be $\sim t^{-0.5}$ for 0.08 and 0.14 Hz channels and $\sim t^{-1}$ for channels 0.28 and higher.

0.08 and 0.14 Hz: Envelopes from the two long period channels are similar, showing a dramatic decrease between 250 and 300-320 seconds (the Rg wave tail, Figure 1a). We observe a small increase between 350 and 450 seconds. This is a long-period ***Lo*** wave. The ***Rg*** tail for the 0.14 Hz channel is weaker than that observed on the 0.08 Hz channel. The increase at 400-450 sec is nearly invisible. The ***Lo*** wave is visible itself, but its coda is not, because of strong attenuation in the upper crust. The uniformly decaying envelope begins at lapse times of 500-550 seconds.

0.28 and 0.32 Hz: Envelopes from these bands differ from those of the long period channels (Figure 1b). ***Rg*** is very weak at these frequencies and no tails are observed. All the wave groups, ***Lg***, ***Rg*** and ***Lo*** are of similar amplitude and little exceed the irregular oscillations before and after them. A very smooth maximum is observed between 270 and 350 seconds, corresponding to a velocity interval from 2.1 to 2.8 km/sec, likely the result of a short-period surface wave ***Lo***, propagating in the upper crust. This wave is usually seen clearly at distances of 200 to 250 km. But because of strong scattering in the upper crust the ***Lo*** waves produce intense coda, then decrease and almost disappear at 750 km. At this distance, the ***Lo*** wave train does not dominate its own coda. This happens owing to strong loss of ***Lo*** energy by both scattering and attenuation processes. This produces a relatively intense coda that attenuates faster than ***Lg*** coda. That is because ***Lg*** travels throughout the entire crust, including the less attenuating lower crust. We conclude that the ***Lo*** coda dominates at lapse-time 400-550 seconds. But then it decreases and after 500-550 seconds the ***Lg*** coda begins to dominate. This conclusion is based on the coda slopes, which differ between 350-500 and 500-1,000 second time ranges. Therefore, we considered two separate codas based on these time limits in this study.

0.62 and 0.67 Hz: At this frequency ***Lg*** is much more intense than ***Lo*** and the coda is associated with the ***Lg*** (Figure 1c). But between 350 and 430 second envelopes flatten, indicating an additional source of scattered waves. This flat portion is, likely, a peak of the ***Lo*** wave, nearly hidden within its own coda. The corresponding arrival time gives a velocity of 1.8-2.1 km/sec. The envelope decay rate between 450 and 1,200 seconds corresponds to a coda Q of 525, which is too high for upper crust propagation. We conclude that at 0.62 Hz the observed coda originated mostly from ***Lg***; only the peak shows above the coda. The coda created from ***Lo*** is mixed with the ***Lg*** coda at times between 350 and 450 seconds.

1.25 and 1.36 Hz: The features we observe in these bands are the similar to those of the 0.62 Hz channel (Figure 1d).

2.5 and 2.9 Hz: These envelopes show a uniform linear decrease from nearly the beginning (300 sec, Figure 1e). The initial part of the envelope, 250 to 300 seconds, consists of a direct ***Lg*** tail. No sign of ***Lo*** exists. We conclude that 2.5 Hz coda originated from high-frequency ***Lg***. Decay slopes differ slightly between 2.5 and 2.9 Hz envelopes.

5 and 5.7 Hz: This high-frequency coda is short and straight, only a few measurements exist beyond 500 seconds, none are recorded at times greater than 550 seconds (Figure 1f).

We summarize our observations as follows: 1) the dominant wave is ***Rg*** at 0.08 and 0.14 Hz, ***Lg*** dominates at 0.62-2.5 Hz and displays a short tail, ***Lo*** dominates at 0.28 Hz and ***Lg*** is nearly invisible and no tail exists at 5 Hz; and 2) the short-period surface wave, ***Lo***, exists on almost all channels from 0.08 to 2.5 Hz, and is seen as a wide weak maximum, exceeding the straight coda envelope by a factor of only 1.2 to 1.7, and we define the beginning of late coda at 500-550 for 0.08 Hz, 450-500 seconds for 0.14-0.28 Hz, 400-450 seconds for 1.25 Hz and 300 seconds for 2.5 and 5 Hz.

We chose the logarithm of the coda envelope at lapse time 500 seconds as a standard measure of coda intensity. These values will be used to construct coda spectra.

Coda Attenuation

We estimate coda Q based on the standard equation (Aki and Chouet, 1975) and results are shown in Table 3. Coda Q was measured separately for earlier and later lapse time intervals for the 0.28 Hz band, as defined above.
We believe that these two intervals represent ***Lo*** and ***Lg*** coda, scattered in the upper crust (***Lo*** coda) and in the whole crust, or, alternatively, in the crust and lithosphere (***Lg*** coda).

Raw Coda Spectra

The coda spectra means the logarithm of the value of coda envelope at lapse time 500 seconds, measured in nm/sec. The spectra were found in a wide frequency band, from 0.08 or 0.14 Hz up to 5.0 Hz, only for large events. For small events the coda exists on only three channels: 0.62-2.5 Hz.

The coda raw spectra of Balapan and Degelen tests are shown in Figures 2a and 2b. The events have a spectral peak with position varying between 0.62 and 1.25 Hz.

In general the Degelen and Balapan spectra are similar, but there are some systematic differences between these two groups. Degelen spectra are a little bit wider than those of Balapan, and have more high frequency energy. These differences are not a result of wave propagation (the volume of scattering media is the same), but are caused by various conditions at the source, and rock properties in these two areas of the Semipalatinsk Nuclear Test Site (STS). The smallest events (down to m = 4.5), with three points of spectrum only, show variable peak positions, either about 1 Hz or less than 0.6 Hz. This indicates a variation in source scaling that might originate with differences in emplacement conditions and that will cause scatter in the observed relationships between high frequency coda amplitude and event magnitude (see below). Generalizing all the spectra into a common scaling law allows us to use deviations of individual spectra from the standard spectra as an indication of source condition.

Table 3. Values of coda Q

Channel, f (Hz)	Qc	in t (sec) interval
0.08	232	550-1400
0.14	252	500-1200
0.28	200	300- 500
0.28	323	500-1400
0.32	180	350- 500
0.32	346	500-1000
0.62	520	450-1100
0.67	525	400-1000
1.25	685	400-950
1.36	625	350- 900
2.5	920	300- 750
2.9	980	300- 600
5	1270	300- 500
5.7	1400	270- 400

Coda Amplitude vs. Magnitude

The relationship between coda amplitudes and magnitude was obtained for each frequency channel. Figure 3 shows examples of such relationships (0.28, 0.62, 1.25 and 2.5 Hz). The magnitudes were taken mostly from AWRE[2] estimates. If AWRE data were not available, we used the mb obtained from energy class values estimated from records of local seismic stations (as described by Khalturin et al. 2001). For each frequency the slope is higher for small events and became lower for large ones. The slope of the relationship decreased with event size, reflecting saturation of the 1-Hz magnitude scale for larger events. At high frequencies (> 1 Hz) the high slope of small events is about 1.33 and the low slope for large events is about 1.0. At low frequencies (f < 1 Hz) the high slope is about 1.0 and the low slope is about 0.65. The change of slope takes place at magnitude about 5.6-5.8 (Figure 4). These relationships can be used to create a scaling law for STS explosions.

[2] AWRE = Atomic Weapons Research Establishment, which includes the British group also known as Blacknest.

Scaling Law of Coda Spectra

To create a scaling law we first estimate the spectrum for a fixed magnitude and then use the set of slopes, dependent on frequency and magnitude, to extrapolate the spectra for several magnitude values. We chose to use m = 5.8 ± 0.25 to obtain the basic spectrum. Events of this size are numerous and their spectra cover our entire frequency range (0.08-5.0 Hz). It is at this magnitude that the slope of coda amplitude vs. magnitude changes. The scaling law obtained was created for all bins of magnitude and frequency for which observed data are available (Figure 5). The scaling law obtained is just a smoothed picture. The most important observations are the individual deviations of real spectra from this averaged one and these remain a focus of our work. We build a common scaling of coda spectra for both Degelen and Balapan events. The individual deviation from this scaling law will be an indication of source conditions of the underground nuclear test.

CONCLUSIONS AND RECOMMENDATIONS

We have manually measured coda envelopes from Talgar ChISS analog records for 124 Semipalatinsk Nuclear Test Site explosions that occurred between 1961 and 1988. These data have been used to study the composition of the coda for the STS-Talgar path, to define coda limits, to estimate coda attenuation, and to construct a scaling law of explosion spectra. Deviations of the coda spectra from the average scaling law could depend on emplacement conditions and will be important to study further. The coda data will be integrated into a coda calibration procedure constructed for use with modern digital data. The ChISS data will be tested for consistency with existing Borovoye digital data from events recorded in common. We anticipate that an adjustment for manual against. Hilbert transform methods of envelope construction will be added to the site correction for these data. If verified, the data will then be useful for yield estimation. The ChISS data set also contains early Lop Nor explosions that are otherwise unavailable and rare, together with STS earthquakes, which will be used to test calibration parameters.

REFERENCES

Aki, K. and B. Chouet (1975). Origin of Coda Waves: Attenuation, and Scattering Effects. *J.Geophys.Res*., 80, 3322-3342.

Khalturin V.I., T.G. Rautian, P.G. Richards (2001). A Study of Small Magnitude Seismic Events During 1961-1989 On and Near the Semipalatinsk Test Site, Kazakhstan, *Pure and Appl. Geoph.*, 158, 143-172.

Rautian, T.G and V.I. Khalturin (1978). The Use of the Coda for Determination of the Earthquake Source Spectrum. *Bull. Seism. Soc. Am*., 68, 923-948.

Tsujiura, M. (1978). Spectral Analysis of the Coda Waves from Local Earthquakes. *Bull. Earthquake Res. Inst*., 53, 1-48.

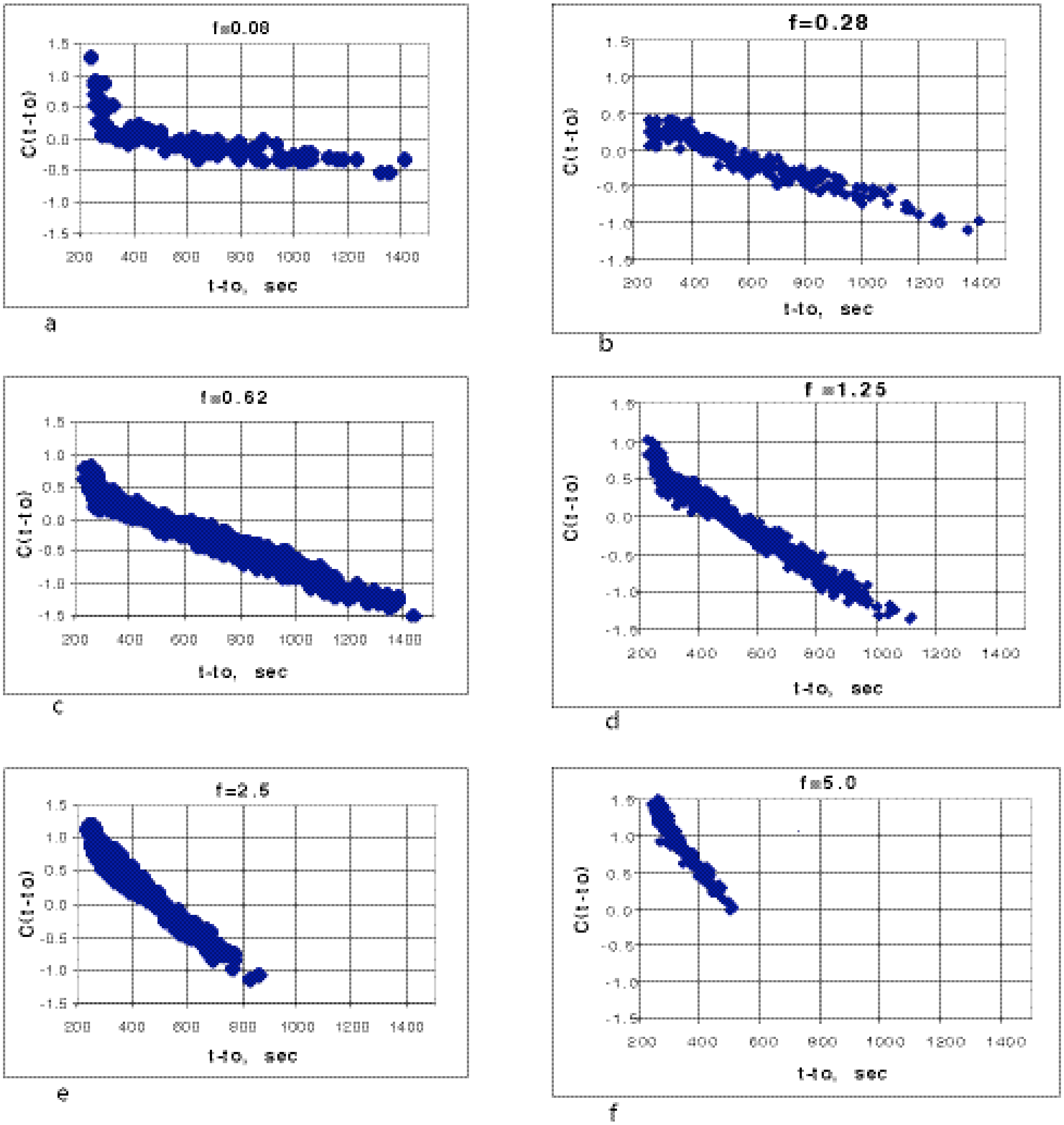

Figure 1. Normalized coda envelopes six channels. (a) 0.08 Hz channel, (b) 0.28 Hz channel, (c) 0.62 Hz channel, (d) 1.25 Hz channel, (e) 2.5 Hz channel, and (f) 5 Hz channel

a

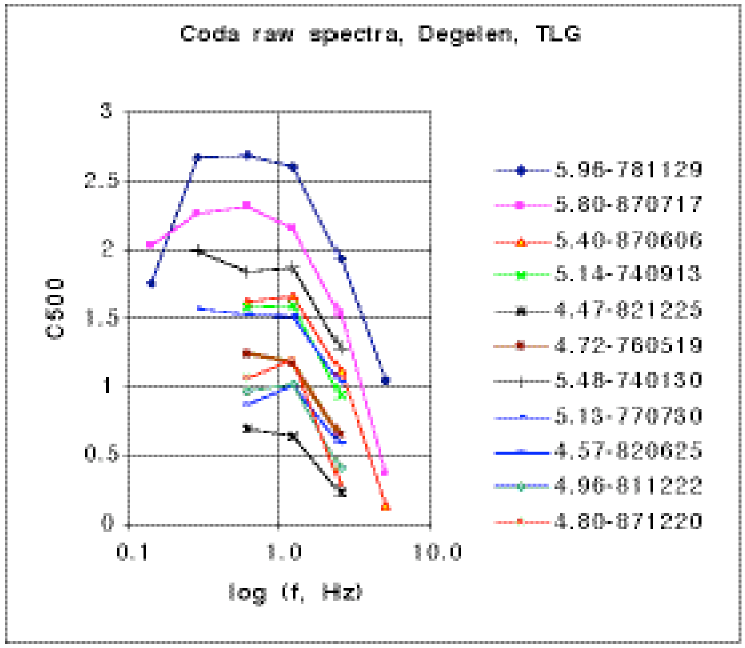

b

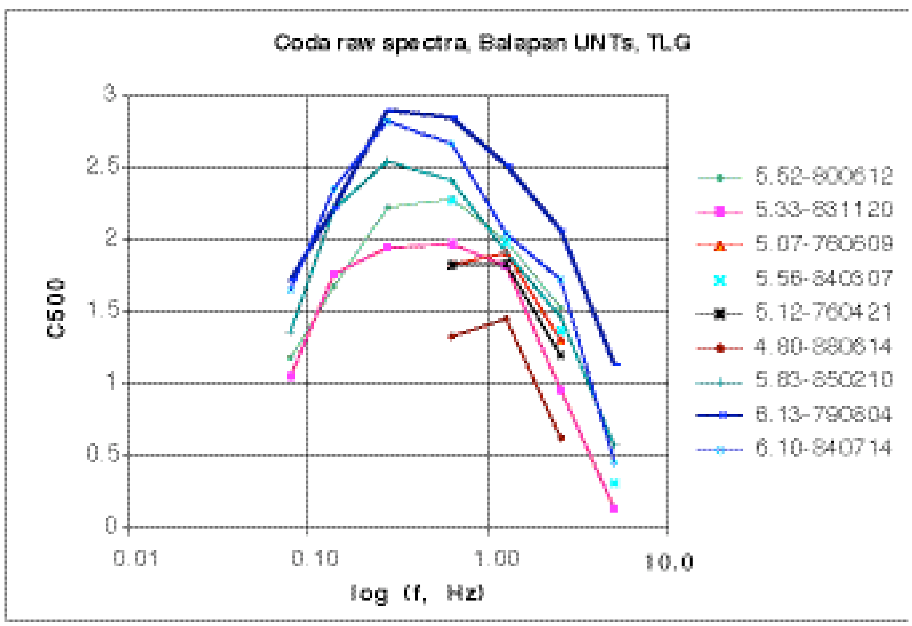

Figure 2. Raw coda spectra, (a) Degelen explosions, and (b) Balapan explosions

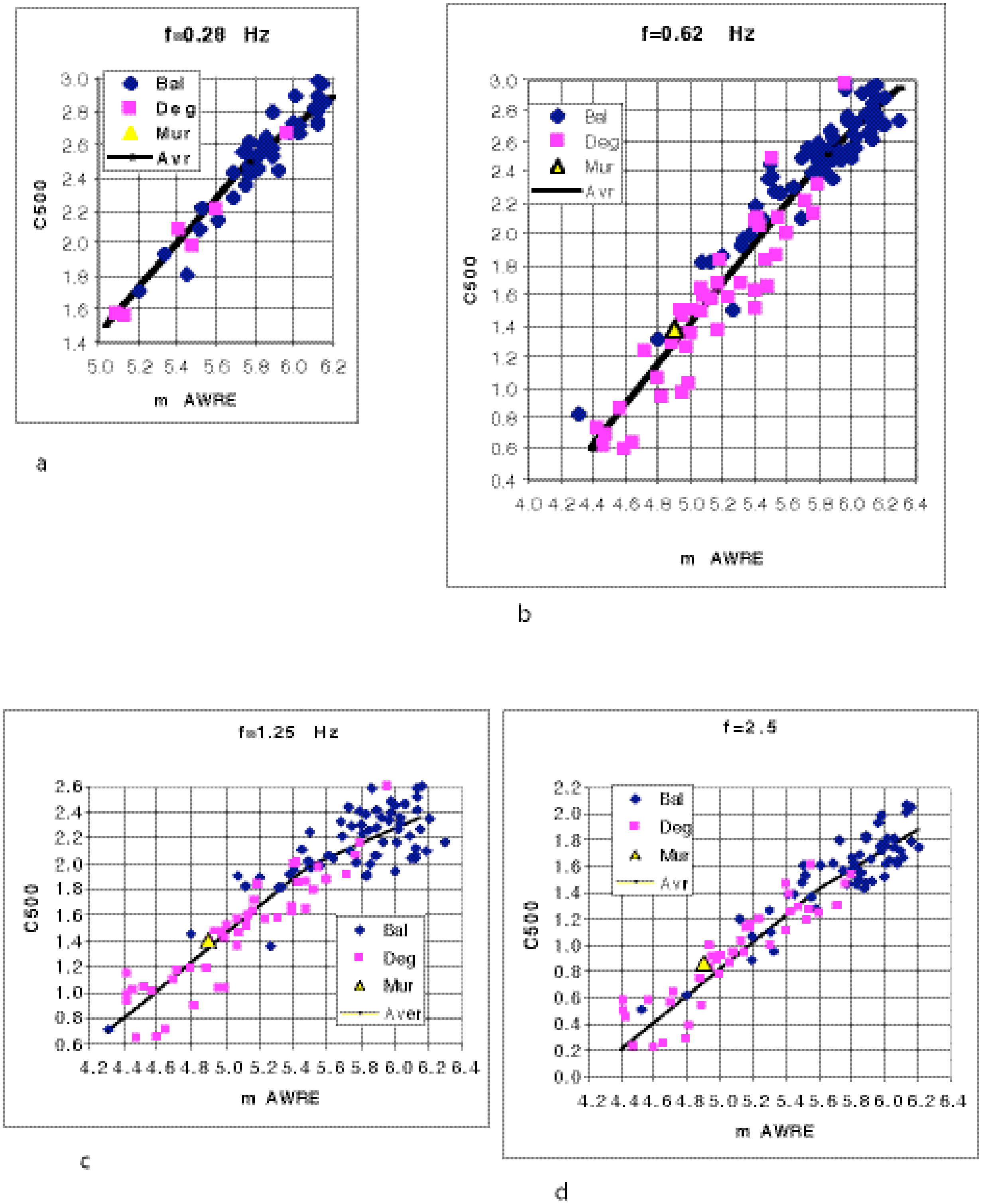

Figure 3. Coda – magnitude relations, (a) f = 0.28 Hz, (b) f = 0.62 Hz, (c) f = 1.25 Hz, and (d) f = 2.5 Hz

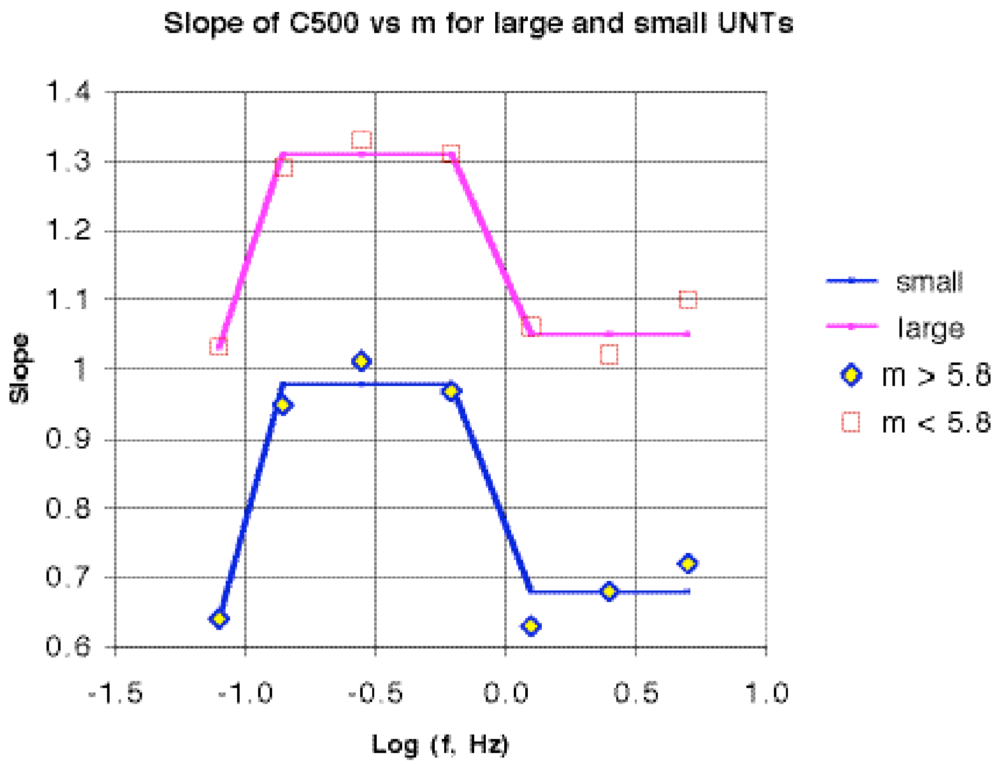

Figure 4. The coda-magnitude slope dependence on magnitude and frequency

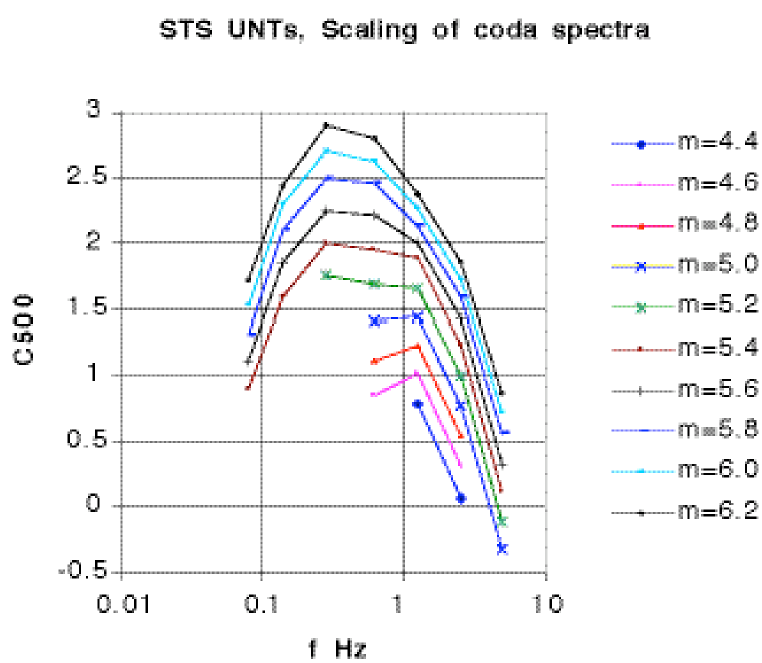

Figure 5. Average scaling of STS UNT coda spectra from Talgar ChISS records